

# Solar activity forecast with a dynamo model

Jie Jiang<sup>1</sup> \*, Piyali Chatterjee<sup>2</sup> and Arnab Rai Choudhuri<sup>1,2</sup>

<sup>1</sup>*National Astronomical Observatories, Chinese Academy of Sciences, Beijing 100012, China.*

<sup>2</sup>*Department of Physics, Indian Institute of Science, Bangalore- 560012, India.*

## ABSTRACT

Although systematic measurements of the Sun’s polar magnetic field exist only from mid-1970s, other proxies can be used to infer the polar field at earlier times. The observational data indicate a strong correlation between the polar field at a sunspot minimum and the strength of the next cycle, although the strength of the cycle is not correlated well with the polar field produced at its end. This suggests that the Babcock–Leighton mechanism of poloidal field generation from decaying sunspots involves randomness, whereas the other aspects of the dynamo process must be reasonably ordered and deterministic. Only if the magnetic diffusivity within the convection zone is assumed to be high (of order  $10^{12} \text{ cm}^2 \text{ s}^{-1}$ ), we can explain the correlation between the polar field at a minimum and the next cycle. We give several independent arguments that the diffusivity must be of this order. In a dynamo model with diffusivity like this, the poloidal field generated at the mid-latitudes is advected toward the poles by the meridional circulation and simultaneously diffuses towards the tachocline, where the toroidal field for the next cycle is produced. To model actual solar cycles with a dynamo model having such high diffusivity, we have to feed the observational data of the poloidal field at the minimum into the theoretical model. We develop a method of doing this in a systematic way. Our model predicts that cycle 24 will be a very weak cycle. Hemispheric asymmetry of solar activity is also calculated with our model and compared with observational data.

**Key words:** Sun: activity, magnetic fields, sunspots

## 1 INTRODUCTION

During the last few decades, solar physicists have attempted to predict the strength of every solar cycle a few years before its onset. When such attempts were made to predict the last cycle 23 in the mid-1990s, there did not yet exist sufficiently sophisticated and detailed models of the solar dynamo. So most of the attempts were primarily based on various precursors which were expected to give an indication of the next solar cycle. Solar dynamo theory has progressed enormously in the last few years and first attempts are now made to predict the next cycle 24 from dynamo models. Dikpati et al. (2006) and Dikpati & Gilman (2006) have predicted that the cycle 24 will be the strongest cycle in 50 years. On the other hand, Choudhuri et al. (2007) have used a different model and different methodology to conclude that the cycle 24 will be the weakest in 100 years. Irrespective of which prediction turns out to be correct, the next cycle 24 should be regarded as a historically important cycle in the evolution of solar dynamo theory—as the first cycle for which detailed dynamo predictions could be made. In view of these

contradictory predictions, it is clear that cycle prediction is a fairly model-dependent affair. Since there are still many uncertainties in solar dynamo models (Choudhuri 2007a), it may be worthwhile to analyze the physical basis of the solar cycle prediction carefully, rather than having too much faith on predictions from any particular model.

Amongst the so-called precursor methods, the most popular method first proposed by Schatten et al. (1978) is to use the polar magnetic field at the preceding minimum as a the precursor for the next maximum. Since the polar field is weak at the present time, Svalgaard et al. (2005) and Schatten (2005) have predicted a weak cycle 24. This prediction is in agreement with the dynamo-based prediction of Choudhuri et al. (2007), but not with the prediction of Dikpati et al. (2006). One important question before us is whether this polar field method is reliable. The next important question is whether dynamo models provide any support for this method.

Since systematic polar field measurements are available only from mid-1970s, we so far have only 3 data points indicating a strong correlation between the polar field at a minimum and the next maximum, as we discuss in the §2. Even if the correlation may appear good, it can be argued that

\* E-mail: jiangjie@ourstar.bao.ac.cn

3 data points do not constitute a good statistics. However, we can use various other proxies like polar faculae (Sheeley 1991) and positions of filaments (Makarov et al. 2001) to infer polar fields from the beginning of the 20th century, and we argue in §2 that there are good reasons to have faith on the polar field method for predicting solar cycles.

We now come to the question whether the polar field method can be justified from dynamo theory. Both the predictions of Dikpati et al. (2006) and Choudhuri et al. (2007; hereafter CCJ) are based on flux transport dynamo models. In these models, the main source of poloidal field is the Babcock–Leighton process in which tilted bipolar regions on the solar surface give rise to a poloidal field after their decay. This poloidal field is advected by the meridional circulation towards the pole, to create a strong (i.e. of order 10 G) polar field at the time of the solar minimum. The conventional wisdom is that this polar field is then advected downward by the meridional circulation to bring it to the tachocline, where it is stretched by the differential rotation to create the toroidal field, ultimately leading to active regions due to magnetic buoyancy. The correlation between the polar field at the minimum and the strength of the next maximum can be explained if this polar field can be brought to the mid-latitude tachocline by the time of the next maximum. Since a maximum comes about 5 years after a minimum, the advection time from the pole to the mid-latitude tachocline has to be of order 5 years if this explanation is to work. Although we do not have any direct observational data on the nature of the meridional circulation in the lower half of the convection zone, the time scale of this circulation seems to set the period of the dynamo (Dikpati & Charbonneau 1999; Hathaway et al. 2003) and we cannot vary the amplitude of the meridional circulation at the bottom of the convection zone too much if we wish to reproduce various observed features of the solar cycle, especially its period. Charbonneau & Dikpati (2000) pointed out that the advection time in their model was of order 20 years and led to a correlation of the polar field at the end of cycle  $n$  with the strengths of the cycles  $n + 2$  and  $n + 3$  rather than the cycle  $n + 1$ . The same is presumably true for the simulations of Dikpati et al. (2006) and Dikpati & Gilman (2006).

In the CCJ model, a sudden change in the polar field at the time of a minimum has a prominent effect on the next maximum coming only after 5 years, as can be seen in Fig. 2 of CCJ. In the caption of Fig. 2, CCJ offered an explanation by suggesting that the advection time in their model was shorter than that in the models of Dikpati and co-workers. We now feel that this explanation was erroneous. When we find two phenomena  $A$  and  $B$  correlated, our first guess usually is that the earlier phenomenon is the cause of the later phenomenon. But an alternative explanation is also possible. If both  $A$  and  $B$  are caused by  $C$  which took place earlier than both  $A$  and  $B$ , then also it is possible for  $A$  and  $B$  to appear correlated. We now believe that the polar field at the minimum and the strength of the next maximum are correlated not because the polar field was the direct cause of the next maximum by being advected from the pole to the tachocline. Rather, they appear correlated because both of them arise from the poloidal field produced by the Babcock–Leighton process in the mid-latitudes. Let us explain this point with Fig. 1.

During a maximum, the poloidal field is created by the

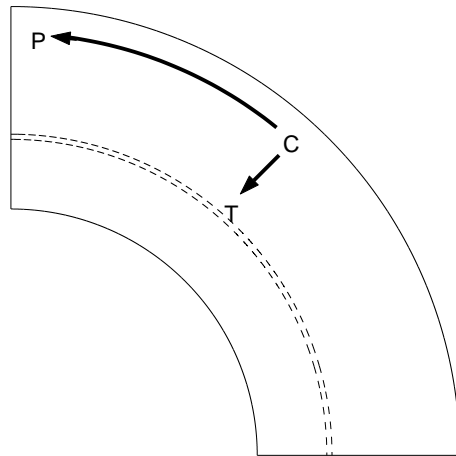


**Figure 1.** A sketch indicating how the poloidal field produced at  $C$  during a maximum gives rise to the polar field at  $P$  during the following minimum and the toroidal field at  $T$  during the next maximum.

Babcock–Leighton process primarily in the region  $C$  indicated in Fig. 1. This field is advected by the meridional circulation to the polar region  $P$  to produce the polar field at the minimum. If diffusion is important, then the poloidal field produced at  $C$  also keeps diffusing. The diffusion in our dynamo model is stronger than in the model of Dikpati and co-workers, as pointed out by Chatterjee et al. (2004) and Chatterjee & Choudhuri (2006). So, in a few years, the poloidal field diffuses from  $C$  to reach the tachocline at  $T$  in our model, which will not happen in the model of Dikpati & Gilman (2006) where the poloidal field will be swept away from  $C$  to  $P$  completely by the meridional circulation before it has any chance to reach the tachocline due to the low diffusivity of that model. Thus, in our model, the poloidal field at  $C$  produced during a maximum gives rise to the polar field at  $P$  during the next minimum and also the toroidal field at  $T$  which is the cause of active regions during the subsequent maximum. The polar field at the minimum and the strength of the next maximum appear correlated not because one is the cause of the other, but because both of them have the poloidal field of the previous cycle as their cause. If the poloidal field produced in the previous cycle was strong, then both of these will be strong, and vice versa.

This brings us to the crucial question as to what determines the strength of the poloidal field produced by the Babcock–Leighton process. CCJ argued that this process involves some randomness and the actual poloidal field produced in the Sun at the end of a cycle will in general be different from the polar field produced in a theoretical mean field dynamo model. The polar field of the theoretical model at the solar minimum will be characteristic of a typical ‘average’ cycle. To model actual cycles, CCJ proposed that the theoretical model should be ‘corrected’ by feeding information about the observed poloidal field at the minimum into the theoretical model in some suitable fashion. CCJ had done this by using the values of DM (Dipole Moment, which is a good measure of the polar field) at the minima computed by Svalgaard et al. (2005). Since values of DM are available only from mid-1970s, this method could be applied to model only the last few solar cycles. While this method yielded re-

sults agreeing reasonably well for cycles 21–23, using only one number like the DM value to characterize the poloidal field at a minimum may seem like a drastic simplification. Especially, if the poloidal field produced all over the surface diffuses through the convection zone to reach the tachocline, then we ought to feed information about poloidal field at all latitudes into our dynamo model rather than feeding only the DM value. One of the aims of this paper is to develop a formalism to do this.

We first discuss in §2 whether the polar fields at minima seem sufficiently well correlated with the strengths of the next maxima on the basis of the observational data. Then a brief description of our dynamo model is provided in §3. Then in §4 we present some calculations done by introducing stochastic fluctuations at the minima in dynamo models with high and low diffusivities to show that a high-diffusivity model provides a better fit with observational data. Several independent arguments in favour of a high magnetic diffusivity are put together in §5. Then in §6 we discuss our methodology of processing the observational data from Wilcox Solar Observatory (WSO) and feeding them into the theoretical dynamo model. Our results based on calculations with more detailed data of poloidal field are presented in §7. We close in §8 with concluding remarks.

## 2 THE IMPLICATIONS OF OBSERVATIONAL DATA

Let us first discuss whether observational data provide good support to the hypothesis that the polar field at the preceding minimum is a reliable precursor for the strength of the next maximum. Table 1 lists the strengths of the last few cycles and the DM values at the minima at the ends of these cycles (only the cycles for which DM values are available are included). The DM values are taken from Svalgaard et al. (2005) as discussed by CCJ. Fig. 1 of Choudhuri (2007b) plotted the strengths of cycles  $n+1$  against the DM values at the ends of cycles  $n$ . Although we have only 3 data points, they lie very close to a straight line implying a strong correlation. These data points are shown by the solid circles in Fig. 2 of this paper. The polar magnetic field of the Sun, which was first detected by Babcock & Babcock (1955) and has been measured occasionally from that time, has been systematically recorded by Wilcox Solar Observatory (WSO) and Mount Wilson Observatory (MWO) from mid-1970s. While we do not have systematic direct measurements of the polar magnetic field at earlier times, the important question is whether we can indirectly infer the values of this field at earlier times and check if the correlation seen in the last 3 cycles also existed in earlier cycles.

We are aware of two works which lead to the possibility of inferring polar fields at earlier times. Sheeley (1991) has compiled the numbers of polar faculae seen in different years in the white-light plates of MWO during the period 1906–1990 and has argued that the polar field strength has a good correlation with the number of polar faculae. The second work which throws light on the evolution of the polar field during 1915–1999 is the work by Makarov et al. (2001), who take the dark filaments seen in white-light plates as indicators of neutral lines where the diffuse magnetic field on the solar surface changes sign. Assuming the positive and nega-

Cycle number	Maximum strength of the cycle $R_{\max}$	DM value at the end of cycle
20	110.6	250
21	164.5	245.1
22	158.5	200.8
23	120.8	119.3

**Table 1.** Maximum strength of the cycle and the DM value at its end are listed against cycle number. The data for this table are taken from Svalgaard, Cliver & Kamide (2005).

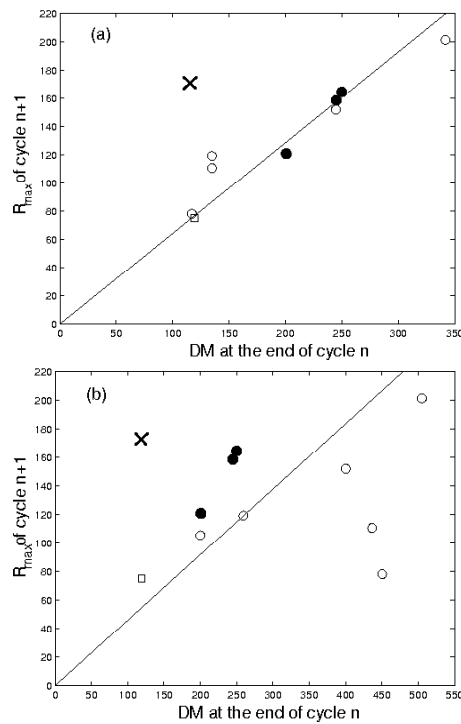


**Figure 2.** Strengths of solar cycles plotted against the DM values of polar fields at the preceding minima. The solid circles are based on actual polar field measurements, whereas the open circles are based on polar fields inferred (a) from values of  $A(t)$  at the minima as given by Makarov et al. (2001), and (b) from the numbers of polar faculae at the minima as given by Sheeley (1991). The points marked by ‘x’ and ‘□’ indicate the data points for cycle 24 according to the models of Dikpati & Gilman (2006) and CCJ.

tive radial magnetic fields on the solar surface to have values +1 G and -1 G respectively, they compute a quantity  $A(t)$  which is a measure of the Sun’s large-scale magnetic field. Since it is the polar field which is the primary source of the Sun’s large-scale magnetic field during the solar minima, values of  $A(t)$  during the minima should be an indicator of the polar field. Both the polar faculae number plotted in Fig. 1 of Sheeley (1991) and  $A(t)$  plotted in Fig. 1 of Makarov et al. (2001) have peaks at the solar minima. These peak values of either faculae number or  $A(t)$  at the successive minima can be taken as measures of the polar field at these minima. Unfortunately the polar fields estimated from the polar faculae number and from  $A(t)$  do not always agree with each other. So one has to be very cautious in using polar field values inferred from either of these data.

For the minima at the ends of cycles 20, 21 and 22, we have DM values available as well as values of  $A(t)$  computed by Makarov et al. (2001). If we divide DM by the peak values of  $A(t)$  at these minima, we get 19.2, 15.8 and 19.1 respectively. Since the average of these is 18.0, we assume that we can multiply peak values of  $A(t)$  at the earlier minima to get the DM values (in  $\mu\text{T}$ ) at these minima. We estimate DM values at the ends of cycles 15–19 in this way. Strengths of cycles  $n + 1$  plotted against these DM values are shown by open circles in Fig. 2(a). The solid circles are based on the actual magnetic field measurements at the ends of cycles 20–22. It seems that there is a very good correlation between the polar field at the end of a cycle and the strength of the following cycle. The points marked by ‘ $\times$ ’ and ‘ $\square$ ’ indicate the data points for cycle 24 according to the models of Dikpati & Gilman (2006) and CCJ. Dikpati & Gilman (2006) predict that cycle 24 will be 30–50% stronger than cycle 23. Since cycle 23 had  $R_{\text{max}} = 120.8$ , this gives a range 157–181 for the  $R_{\text{max}}$  value of cycle 24, with an average of 169. We have used this value in Fig. 2(a).

If we use the peak polar faculae numbers as given in Fig. 1 of Sheeley (1991) to estimate the polar fields at the minima, then the correlation turns out to be considerably worse. This is shown in Fig. 2(b). The open circles in this figure are obtained by assuming that the DM values (in  $\mu\text{T}$ ) at the minima are given by multiplying the total number of polar faculae (i.e. the sum of north and south polar faculae) by a factor 4.55. This is done for the minima at the ends of cycles 14–19, whereas the solid circles are based on actual polar field measurements at the ends of cycles 20–22. The correlation would have looked considerably better if two data points at the bottom right did not exist. These two data points correspond to the minima around 1923 and 1964. These minima were followed by the two weakest cycles in the past century. According to Fig. 1 of Sheeley (1991), the polar faculae counts during these minima were reasonably high, suggesting that the polar fields would have been strong and thus offsetting the two data points in Fig. 2(b). On the other hand, values of  $A(t)$  at these minima, as shown in Fig. 1 of Makarov et al. (2001), were quite low. This suggests weaker magnetic fields at these minima, which would bring the two data points much closer to the correlation line. We shall probably never know for sure whether the polar fields at these minima were actually weak or strong. This shows that using other parameters as proxies of the polar field can be problematic. Only when we have reliable polar magnetic measurements for several cycles, we shall be able to determine really how good a correlation exists between the polar fields at the minima and the strengths of the next cycles. Errors in the polar field estimate probably make the correlation look worse than what it actually is. For example, if we had actual polar field measurements for the two data points at the bottom right of Fig. 2(b), probably these points would lie closer to the correlation line. In spite of various uncertainties, Figs. 2(a) and 2(b) suggest that the correlation between the polar field at a minimum and the strength of the next maximum is reasonably good. It may be noted that Makarov et al. (1989) found a correlation between the polar faculae number and the sunspot number about 6 years later.

Fig. 3 plots the DM values of the polar field at the ends of cycles against the strengths of those cycles. Again, the 4 solid circles are based on actual polar field measure-

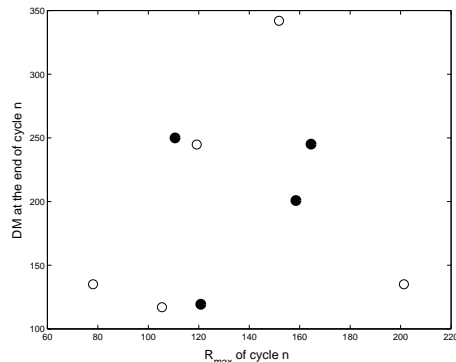


**Figure 3.** DM values of polar fields at the minima plotted against the strengths of the previous solar cycles. The solid circles are based on actual polar field measurements, whereas the open circles are based on polar fields inferred from values of  $A(t)$  at the minima as given by Makarov et al. (2001).

ments, whereas the 5 open circles are based on DM values inferred from  $A(t)$  peak values. Neither the solid circles, nor the open circles show much correlation. It is clear that the strength of a cycle does not determine the polar field produced at the end of the cycle, implying that the generation of the poloidal field involves randomness. The lack of correlation in Fig. 3 can be taken as a justification behind the assumption of CCJ that the polar field at the end of a cycle cannot be inferred from the sunspot data of the cycle and has to be fed into the theoretical model by using actual observational data. On the other hand, Dikpati & Gilman (2006) have used the sunspot area data as the completely deterministic source of poloidal field in their model. According to our judgment, it is wrong to assume a process which clearly involves randomness and is poorly correlated to be deterministic. Using suitably averaged sunspot area data, Cameron & Schüssler (2007) found a rather intriguing correlation between the theoretically computed magnetic flux crossing the equator at the minimum and the strength of the next maximum, for the last few cycles. They suggested this as a possible reason how Dikpati & Gilman (2006) “predicted” the past cycles. However, this correlation virtually disappeared when Cameron & Schüssler (2007) used more detailed sunspot data rather than the smoothed data.

### 3 THE STANDARD DYNAMO MODEL

The toroidal field of the dynamo is universally believed to be produced in the tachocline. A very influential idea for the generation of the poloidal field is the  $\alpha$ -effect, which assumes that the toroidal field is twisted by helical turbulence to give rise to the poloidal field (Parker 1955; Steenbeck et al. 1966). When flux tube rise simulations established that the toroidal field at the bottom of the solar convection zone (hereafter SCZ) has to be much stronger than the equipartition field (Choudhuri & Gilman 1987; Choudhuri 1989; D’Silva & Choudhuri 1993; Fan et al. 1993), it became clear that the traditional  $\alpha$ -effect will be suppressed. This has led several dynamo theorists in recent years to invoke an alternative idea of poloidal field generation from the decay of tilted active regions proposed by Babcock (1961) and

Leighton (1969). The meridional circulation, which is poleward near the surface and equatorward at the bottom of SCZ, has to play an important role in such dynamo models called ‘flux transport dynamos’ (Wang et al. 1991). Two-dimensional flux transport dynamo models were first constructed by Choudhuri et al. (1995) and Durney (1995).

Most of our calculations are based on the dynamo model presented by Nandy & Choudhuri (2002) and Chatterjee et al. (2004). The readers are advised to consult either Chatterjee et al. (2004) or Choudhuri (2005) for the full details of the model. Here we present only the salient features. The basic equations for the standard axisymmetric  $\alpha\Omega$  solar dynamo model are

$$\frac{\partial A}{\partial t} + \frac{1}{r \sin \theta} (\mathbf{v} \cdot \nabla) (r \sin \theta A) = \eta_p \left( \nabla^2 - \frac{1}{r^2 \sin^2 \theta} \right) A + \alpha B, \quad (1)$$

$$\frac{\partial B}{\partial t} + \frac{1}{r} \left[ \frac{\partial}{\partial r} (r v_r B) + \frac{\partial}{\partial \theta} (v_\theta B) \right] = \eta_t \left( \nabla^2 - \frac{1}{r^2 \sin^2 \theta} \right) B + r \sin \theta (\mathbf{B}_p \cdot \nabla) \Omega + \frac{1}{r} \frac{d\eta_t}{dr} \frac{\partial}{\partial r} (rB), \quad (2)$$

where  $B(r, \theta, t)\mathbf{e}_\phi$  and  $\nabla \times [A(r, \theta, t)\mathbf{e}_\phi]$  respectively correspond to the toroidal and poloidal components. Here  $\mathbf{v}$  is the meridional flow,  $\Omega$  is the internal angular velocity and  $\alpha$  describes the generation of poloidal field from the toroidal field. The turbulent diffusivities for the poloidal and toroidal field are denoted by  $\eta_p$  and  $\eta_t$ . Since turbulence has less effect on the stronger toroidal field, we in principle allow  $\eta_p$  and  $\eta_t$  to be different. Magnetic buoyancy is treated by removing a part of  $B$  from the bottom of SCZ to the top whenever  $B$  exceeds a critical value, as discussed by Chatterjee et al. (2004, §2.6). Such a treatment of magnetic buoyancy coupled with  $\alpha$  concentrated at the top of SCZ captures the essence of the Babcock–Leighton process of poloidal field generation (Nandy & Choudhuri 2001). Although the period of a flux transport dynamo is determined mainly by the meridional flow speed (Dikpati & Charbonneau 1999; Hathaway et al. 2003) and this flow speed is known to vary, the detailed time variation is known only since 1996 (Gizon 2004). Hence, we adopt a steady meridional flow speed. Chatterjee et al. (2004, §2) and Choudhuri (2005) describe how the various parameters  $\mathbf{v}$ ,  $\Omega$ ,  $\eta_p$ ,  $\eta_t$  and  $\alpha$  were specified to produce what they called their *standard* model, of which the solution was presented in §4 of Chatterjee et al. (2004). The period of this standard model was about 14 years. We change  $\mathbf{v}$  along with some other parameters to get a period of 10.8 years. The old values and the changed values of the parameters are listed in Table 1. The dynamo model with the changed values giving a period of 10.8 years is referred to our *standard1* model. Most of our high-diffusivity calculations in this paper are done with this *Standard1* model.

Since the diffusion of the poloidal field is going to play a very important role, we write down the expression of  $\eta_p$  which we use, although the reader is referred to Chatterjee et al. (2004) or Choudhuri (2005) for the expressions of the other parameters. We take  $\eta_p$  to be given by

$$\eta_p(r) = \eta_{RZ} + \frac{\eta_{SCZ}}{2} \left[ 1 + \operatorname{erf} \left( \frac{r - r_{BCZ}}{d_t} \right) \right]. \quad (3)$$

Here  $\eta_{SCZ}$  is the turbulent diffusivity inside the convection zone, which is taken as  $2.4 \times 10^{12} \text{ cm}^2 \text{ s}^{-1}$  in the *Standard1* model. The diffusivity  $\eta_{RZ}$  below the bottom of SCZ is as-

**Table 2.** The original values of the parameters in the standard model (§4 of Chatterjee et al. 2004) along with the changed values we use now. The first four parameters control the amplitude, penetration depth, equatorial return flow thickness and the position of the inversion layer of the meridional circulation, respectively. The half width of tachocline is denoted by  $d_{tac}$ .

Parameter	Standard Model	This Model
$v_0$	$-29 \text{ m s}^{-1}$	$-35 \text{ m s}^{-1}$
$R_p$	$0.61 R_\odot$	$0.63 R_\odot$
$\alpha_0$	$25 \text{ ms}^{-1}$	$22.5 \text{ ms}^{-1}$
$\beta_2$	$1.8 \times 10^{-8} \text{ m}^{-1}$	$1.3 \times 10^{-8} \text{ m}^{-1}$
$r_0$	$0.1125 R_\odot$	$0.1184 R_\odot$
$d_{tac}$	$0.025 R_\odot$	$0.015 R_\odot$

sumed to have a rather value of  $2.2 \times 10^8 \text{ cm}^2 \text{ s}^{-1}$ . A plot of  $\eta_p$  can be seen in Fig. 4 of Chatterjee et al. (2004).

We carry on our calculations with the solar dynamo code *Surya* developed at the Indian Institute of Science. This code and a detailed guide (Choudhuri 2005) for using it are made available to anybody who sends a request to Arnab Choudhuri (e-mail address: arnab@physics.iisc.ernet.in). This code has not only been used for doing several dynamo calculations (Nandy & Choudhuri 2002; Chatterjee et al. 2004; Choudhuri et al. 2004; Chatterjee & Choudhuri 2006; CCJ), a modified version of the code has also been used to study the magnetic field evolution in neutron stars (Choudhuri & Konar 2002; Konar & Choudhuri 2004).

A flux transport dynamo combines three basic process: (i) the strong toroidal field  $B$  is produced by the stretching of the poloidal field by differential rotation  $\Omega$  in the tachocline; (ii) the toroidal field generated in the tachocline rises due to magnetic buoyancy to produce sunspots (active regions) and the decay of tilted bipolar sunspots produces the poloidal field  $A$  by the Babcock–Leighton mechanism; (iii) the meridional circulation  $\mathbf{v}$  advects the poloidal field first to high latitudes and then down to the tachocline at the base of the convection zone, although we are now suggesting that diffusivity may play a more significant role than meridional circulation in bringing the poloidal field to the tachocline in high-diffusivity models. CCJ argued that the processes (i) and (iii) are reasonably ordered and deterministic, whereas the process (ii) involves an element of randomness, which presumably is the primary cause of solar cycle fluctuations. Firstly, although active regions appear in a latitude belt at a certain phase of the solar cycle, where exactly within this belt the active regions appear seems random. Secondly, there is considerable scatter in the tilts of bipolar active regions around the average given by Joy’s law (Wang & Sheeley 1989). The action of the Coriolis force on the rising flux tubes gives rise to Joy’s law (D’Silva & Choudhuri 1993), whereas convective buffeting of the flux tubes in the upper layers of the convection zone causes the scatter of the tilt angles (Longcope & Fisher 1996; Longcope & Choudhuri 2002). Since the poloidal field generated from an active region by the Babcock–Leighton process depends on the tilt, the scatter in the tilts introduces a randomness in the poloidal field generation process. We suggest that the poloidal field at the solar minimum produced in a mean field dynamo model is some kind of ‘average’ poloidal field dur-

ing a typical solar minimum. The poloidal field during a particular solar minimum may be stronger or weaker than this average field. By feeding the observational data into the model, we have to correct the ‘average’ poloidal field to make the prediction of the next cycle.

CCJ corrected the average poloidal field at a minimum by the very simple method of changing the values of  $A$  above  $0.8R_{\odot}$  in accordance with the DM value at that minimum. The advantage of this method is that it is extremely easy to implement. It is, however, a drastic over-simplification to represent the poloidal field at the minimum by a single number. Especially, in the high-diffusivity models, if the poloidal field diffuses downward at different latitudes instead of being advected to the pole first, then it may be important to develop a methodology of feeding values of poloidal field at different latitudes into the theoretical model instead of using only the value of DM. Wilcox Solar Observatory (WSO) has regularly measured the line-of-sight component of the magnetic field using the  $5250 \text{ \AA}$  Fe I line since the later part of 1976. This component can be taken as a simple projection of the radial field. We will discuss in §6 how to analysis WSO data and connect them with our dynamo model. We would like to point out that the quality of the data should be sufficiently high to ensure that our methodology gives meaningful results. In §7 we shall present our results obtained with WSO data. When we tried to use the data from National Solar Observatory (NSO), we were completely unable to model the past cycles properly. Before we present the results obtained with detailed poloidal field data, we use the simpler method of CCJ for updating the poloidal field in the next section to highlight the differences between dynamo models with high and low diffusivities.

Even before the development of realistic flux transport dynamo models, Choudhuri (1992) suggested that the stochastic fluctuations around the mean values of various quantities may be the source of irregularities in the solar cycle. This idea was further explored by several other authors (Moss et al. 1992; Hoyng 1993; Ossendrijver et al. 1996; Mininni & Gomez 2002). Now we identify the randomness in the Babcock–Leighton process as the source of stochastic fluctuations in the solar dynamo.

#### 4 CONTRASTING BEHAVIOURS OF DYNAMOS WITH HIGH AND LOW DIFFUSIVITIES

In §2 we have seen that there is reasonably convincing observational evidence that the strength of the polar field at a minimum plays an important role in determining the strength of the next maximum coming about 5 years later. The results of CCJ reproduce this observed pattern. Fig. 1 of the present paper and the accompanying text explains how this happens. It is the poloidal field cumulatively generated during the declining phase of the cycle which is responsible for both the polar field at the end of the cycle (produced by poleward advection of this poloidal field from mid-latitudes) and the maximum of the next cycle (since the toroidal field is generated from this poloidal field which has diffused to the bottom of the convection zone). To support our assertion, the left column of Fig. 4 shows how the poloidal field lines evolve in our *Standard1* model with diffusivity on the

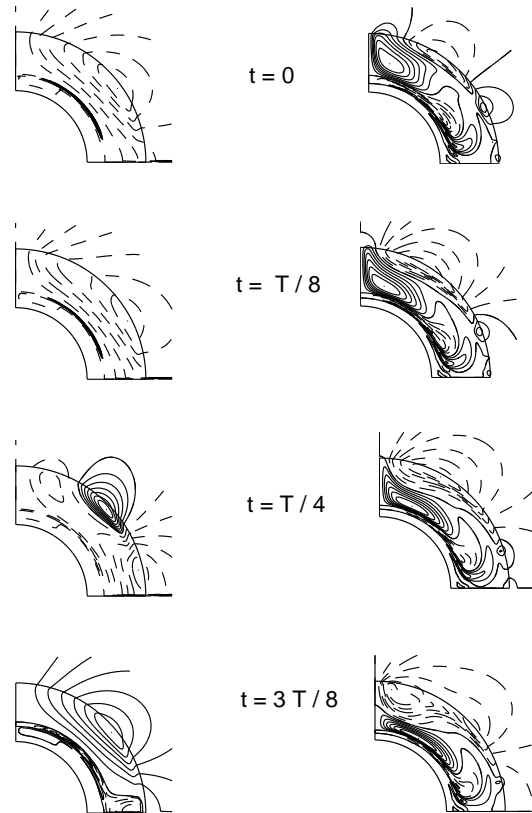


**Figure 4.** Evolution of the poloidal field. The left column corresponds to our high-diffusivity *Standard1* model. The right column corresponds to the low-diffusivity model of Dikpati & Charbonneau (1999), except that we have taken  $u_0 = 20 \text{ m s}^{-1}$ .

higher side. For the sake of comparison, the right side of Fig. 4 shows the poloidal field evolution in a low-diffusivity model, which we shall discuss later. Since we are not concerned with parity issue here, most of the calculations in this Section are done in a hemisphere with boundary conditions at the equators appropriate for a dipolar solution.

We have seen in Fig. 2 of CCJ that, if the poloidal field above  $0.8R_{\odot}$  is suddenly changed at a minimum, then the maximum coming soon after that and the subsequent maximum are both affected. From this, we expect that the strength of a maximum should depend on the polar field strengths at the two preceding minima. Thus, while the polar field at the immediately preceding minimum should not determine the strength of the maximum completely, we expect our theoretical model to show a good correlation between the polar field of a minimum and the strength of the next maximum, as we see in the observational data discussed in §2. Since the poloidal field generated at the surface has to diffuse to the tachocline in a few years to produce this correlation, we expect that the correlation will get worse if the diffusivity is reduced. We carry out some numerical experiments to test this.

We run our dynamo code for several cycles, stopping it at every minimum and changing the value of  $A$  above  $0.8R_{\odot}$  in the following fashion. We use a random number generating programme to generate random numbers between 0.5 and 1.5. We take one of these random numbers as the factor  $\gamma$  for a minimum and multiply  $A$  above  $0.8R_{\odot}$  by a con-

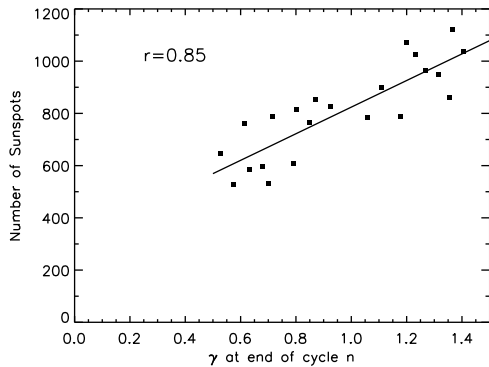


**Figure 5.** The strength of the maximum of cycle  $n + 1$  plotted against the randomly chosen value of  $\gamma$  at the end of cycle  $n$ . *Standard1* model is used to generate this plot.

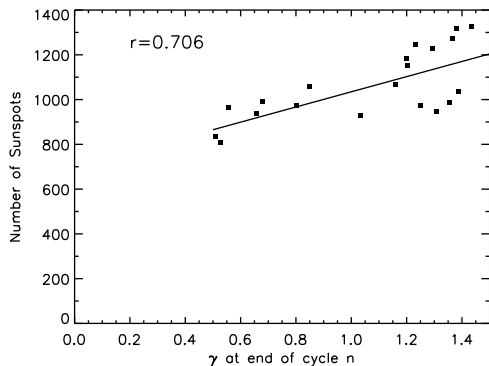


**Figure 6.** The strength of the maximum of cycle  $n + 1$  plotted against the randomly chosen value of  $\gamma$  at the end of cycle  $n$ . The diffusivity  $\eta_P$  is made half its value used in the *Standard1* model to generate this plot.

stant number such that the amplitude of the poloidal field becomes  $\gamma$  times the amplitude of the poloidal field produced in an average cycle (i.e. when the code is run without any interruptions). Fig. 5 plots the strengths of the next maxima against values of  $\gamma$  chosen in the preceding minima (which can be regarded as indicative of the strengths of the polar field at the minima). We see a very good correlation as we see in the observational data of Fig. 2. Then we repeat this numerical experiment by reducing the diffusivity of the poloidal field within the convection zone to half its value, i.e.  $\eta_{SCZ}$  is changed from the value  $2.4 \times 10^{12} \text{ cm}^2 \text{ s}^{-1}$  used in our *Standard1* model to the value  $1.2 \times 10^{12} \text{ cm}^2 \text{ s}^{-1}$ . All the other parameters are kept the same, except we change  $\alpha_0$  to  $9 \text{ m s}^{-1}$  to make sure that the solutions remain oscillatory. The run with this reduced diffusivity gives Fig. 6, where we find the correlation to be worse than what it is in Fig. 5. It is thus clear that reducing the diffusivity in the theoretical model leads to worsening of the correlation between the polar field at the minimum and the strength of the next maximum. However, Fig. 6 still represents a case in which the poloidal field reaches the tachocline by diffusing from the surface in a few years. If we really want to make diffusion inefficient such that the poloidal field cannot reach

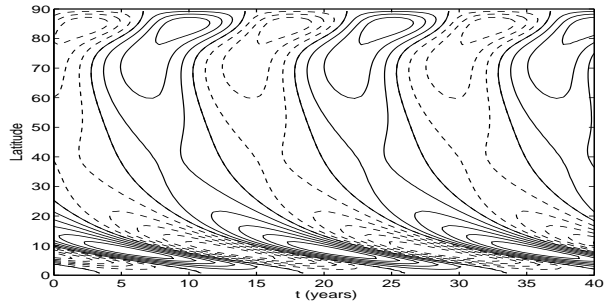


**Figure 7.** The theoretical butterfly diagram obtained with our code *Surya* for the low-diffusivity model of Dikpati & Charbonneau (1999), except that we have taken  $u_0 = 20 \text{ m s}^{-1}$ .

the tachocline by diffusion and has to be advected there by the meridional circulation, then we have to reduce the diffusivity of the poloidal component in our model by at least one order of magnitude. As it happens, our model does not give oscillatory solutions if the diffusivity of the poloidal field in the convection zone is reduced by a factor of 10 while keeping the other parameters unchanged. We, therefore, carry on some tests on the model of Dikpati & Charbonneau (1999) to study the behavior of a dynamo with low diffusivity.

Dikpati & Charbonneau (1999) present what they call a ‘reference solution’ in §3 of their paper. The turbulent diffusivity within the convection zone in this solution is taken to be  $5 \times 10^{10} \text{ cm}^2 \text{ s}^{-1}$ , which is about 50 times smaller than the value we use in our *Standard1* model. We try to reproduce this reference solution with our dynamo code *Surya* by changing the various parameters to what are given in the paper of Dikpati & Charbonneau (1999). Especially, we change the form of the meridional circulation to the form proposed by van Ballegoijen & Choudhuri (1988), which has been used by Dikpati & Charbonneau (1999). We also treat the magnetic buoyancy in the non-local way as they have done. We found that our solution had a longer period and looked somewhat different from the solution presented in Fig. 3 of Dikpati & Charbonneau (1999). However, when we take the amplitude of the meridional circulation to be  $u_0 = 20 \text{ m s}^{-1}$  rather than  $u_0 = 10 \text{ m s}^{-1}$  as quoted by Dikpati & Charbonneau (1999), we get the theoretical butterfly diagram shown in Fig. 7, which very closely resembles Fig. 3 of Dikpati & Charbonneau (1999). The evolution of the poloidal field in this model has been shown on the right side of Fig. 4. This can be compared with the plots given on the right side of Fig. 2 of Dikpati & Charbonneau (1999). Again we find that our plots look very similar to theirs. It thus appears that our code *Surya* is capable of reproducing the results of Dikpati & Charbonneau (1999).

Comparing with the high-diffusivity solution shown on the left side of Fig. 4, we find that the poloidal field in this low-diffusivity solution is not able to diffuse to the tachocline from the surface, but is advected there by the meridional circulation. Taking the diffusion time to be  $L^2/\eta$  where  $L$  is the depth of the convection zone, the diffusion time in the low-diffusivity model is larger than 250 years, but is of order 5 years in the high-diffusivity *Standard1* model. In the low-diffusivity solution, when the poloidal field produced in a cycle is being brought to the tachocline, the poloidal field produced in the earlier cycles are still present at the

bottom of the convection zone, which is not the case in the high-diffusivity solution where poloidal fields produced in the earlier cycles decay away more quickly. In the low-diffusivity case, we expect the polar field to have an effect on the sunspot production only when it is advected to the tachocline after a time lag. We now carry on the same numerical experiment on this low-diffusivity model as we did on our high-diffusivity model, by stopping the code at every minimum and changing  $A$  above  $0.8R_{\odot}$  by multiplying it by a random number as we had done to produce Figs. 5–6. The result for the Dikpati–Charbonneau model (with  $u_0$  taken as  $20 \text{ m s}^{-1}$ ) is shown in Fig. 8, with the two panels plotting the strengths of the cycle  $n+1$  and  $n+3$  respectively against the value of  $\gamma$  at the end of the cycle  $n$ . As expected, there is no correlation in this case between the polar field at the minimum and the strength of the next maximum occurring only a few years later, since the polar field would take a longer time to be advected to the region in the tachocline where sunspots are produced. We, however, find a very weak correlation between the polar field and the strength of the third next cycle. It may be pointed out that Charbonneau & Dikpati (2000) carried out a study by introducing stochastic fluctuations in the model of Dikpati & Charbonneau (1999). In order to generate sunspot number plots, Charbonneau & Dikpati (2000) took the magnetic energy in the tachocline at a latitude of  $15^\circ$  to be indicative of the sunspot number. To estimate the strengths of maxima for producing Fig. 8, we have followed the same procedure. Fig. 9 of Charbonneau & Dikpati (2000) presented correlations of the polar field with the next few maxima on introducing stochastic fluctuations. They also found that the polar field was not correlated with the next maximum and the strongest correlation was obtained with the third maximum.

We now carry on the same numerical experiment with this low-diffusivity model as what had been done by CCJ to produce their Fig. 2. At a minimum, we change  $A$  above  $0.8$  by multiplying it by  $2.0$  and  $0.5$  respectively. Then we run the code without further interruptions. Fig. 9 shows the sunspot number plot (i.e. the plot of magnetic energy in the tachocline at latitude  $15^\circ$ ). We find that a change in the polar field during the minimum has no effect on the next maximum, has a small effect on the maximum after that and a much bigger effect on the third maximum. This is consistent with the result of Charbonneau & Dikpati (2000, Fig. 9) that the polar field had the strongest correlation with the third maximum. Apart from the important point that the polar field at a minimum does not seem to have an effect on the next maximum in a low-diffusivity model, even the effect on the next two maxima is somewhat smaller than the effect on the next maximum that we see in Fig. 2 of CCJ. It may be noted that Charbonneau & Dikpati (2000) had to introduce fluctuations as large as 200% in their poloidal field source term in order to get any noticeable effect. It thus seems that low-diffusivity models not only introduce an unrealistically large time delay inconsistent with observations, they also require very large fluctuations in the polar field to produce appreciable effects on the dynamo.

The solar cycle prediction work of Dikpati & Gilman (2006) is based on the ‘calibrated’ flux transport dynamo model presented by Dikpati et al. (2004). It was our intention to do some tests on this model. So we tried to reproduce this model with our code *Surya*. We found some obvious ty-

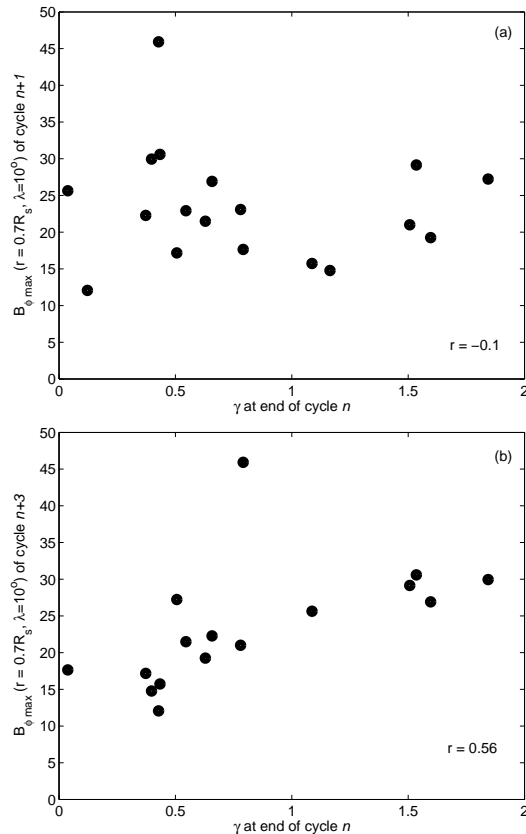


**Figure 8.** The strength of the maximum of (a) cycle  $n+1$  and (b) cycle  $n+3$  plotted against the randomly chosen value of  $\gamma$  at the end of cycle  $n$ . These plots are obtained from the low-diffusivity model.

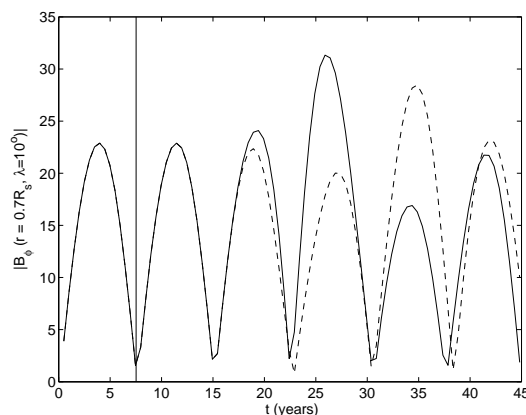


**Figure 9.** Sunspot number plots by increasing (solid line) and decreasing (dashed line) the poloidal field by 50% above  $0.8R_{\odot}$  at a solar minimum (indicated by the vertical line). These plots are based on the low-diffusivity model.

pographical errors in the specification of the parameters as given in Dikpati et al. (2004), which were corrected (in consultation with Dr. Dikpati). These typographical errors have now been listed by Dikpati & Gilman (2007). Apart from these typographical corrections, we put in our code the exactly same expressions of meridional circulation, turbulent diffusivity and  $\alpha$ -coefficient as used by Dikpati et al. (2004)



with the same values of different parameters. We also ran the code in a full sphere rather than in a hemisphere as done in the case of the other calculations in this section, to make sure that all the conditions (after correcting the typographical errors) were identical with the conditions used by Dikpati et al. (2004) to produce their ‘calibrated’ solution. We found a decaying solution, in contrast to the oscillatory solution which Dikpati et al. (2004) reported. Although our code reproduces the results of Dikpati & Charbonneau (1999), the results reported in Dikpati et al. (2004) are not reproduced. That is the reason why we had to use the model of Dikpati & Charbonneau (1999) when we wanted to do some tests on a low-diffusivity model.

It may be noted that Nandy & Choudhuri (2002) argued that a meridional circulation penetrating slightly below the tachocline is needed to produce solar-like butterfly diagrams and we are using such a circulation. Dikpati & Charbonneau (1999) and Charbonneau & Dikpati (2000) also used such penetrating circulation (see Fig. 2 in Choudhuri et al. 2005). Dikpati et al. (2004) are the only authors to claim that they can get solar-like butterfly diagrams, with sunspots confined to low latitudes, even with a non-penetrating meridional circulation. This result has so far not been reproduced by any other group. Other groups using non-penetrating circulation have always obtained butterfly diagrams extending to fairly high latitudes (Bonanno et al. 2002; Guerrero & de Gouveia Dal Pino 2007). It remains to be seen whether any other dynamo group is able to reproduce the model of Dikpati et al. (2004), which we cannot reproduce with our dynamo code and on which the predictions of Dikpati & Gilman (2006) are based.

## 5 ARGUMENTS IN FAVOUR OF HIGH DIFFUSIVITY OF THE POLOIDAL FIELD

From the results presented in the previous section, it should be clear that the diffusivity in the convection zone has to be high if the polar field at the minimum has to be correlated with the strength of the next maximum as seen in the observational data. This is a very compelling argument that the turbulent diffusivity of the convection zone is probably high like  $2 \times 10^{12} \text{ cm}^2 \text{ s}^{-1}$  as taken in our model (Chatterjee et al. 2004; CCJ) and not low like  $5 \times 10^{10} \text{ cm}^2 \text{ s}^{-1}$  as taken in the models of Dikpati and her collaborators (Dikpati & Charbonneau 1999; Charbonneau & Dikpati 2000; Dikpati et al. 2004; Dikpati & Gilman 2006). We now list several other arguments in support of a high diffusivity.

(i) Even if we assume the turbulent velocities within the SCZ to have rather low values like  $v \approx 10 \text{ m s}^{-1}$  and the convection cells to have rather small sizes like  $l \approx 30,000 \text{ km}$ , still the turbulent diffusivity  $\approx (1/3)vl$  would turn out to be not less than  $10^{12} \text{ cm}^2 \text{ s}^{-1}$ . Thus simple order-of-magnitude estimates favour the high values of diffusivity that we use rather than the low values used by Dikpati and her co-workers. Parker (1979, p. 629) used the convection zone model of Spruit (1974) to conclude that the turbulent diffusivity should be of order  $1\text{--}4 \times 10^{12} \text{ cm}^2 \text{ s}^{-1}$  within the convection zone. It may be noted that convection zone dynamo models developed in the early years of solar dynamo research gave best results when the turbulent diffusivity was taken to be of order  $10^{12} \text{ cm}^2 \text{ s}^{-1}$  (Köhler 1973; Moffatt

1978, §9.12). Interface dynamos, however, required smaller diffusivities of order  $10^{10} \text{ cm}^2 \text{ s}^{-1}$  to match the observed period of the solar cycle (Choudhuri 1990).

(ii) Wang et al. (1989) studied the evolution of the diffuse magnetic field on the solar surface under the joint influence of diffusion and meridional circulation. They concluded that theory fits observations best if diffusivity at the solar surface is taken to be  $10^{12} \text{ cm}^2 \text{ s}^{-1}$  or larger, comparable to the diffusivity within convection zone used in our model. While the surface value of diffusivity inferred by Wang et al. (1989) may not necessarily imply that diffusivity inside the convection zone also has to be comparable, it is still worth noting that the value of diffusivity used by us is so comparable to what is needed to match surface observations. This surface value of turbulent diffusion also follows from the fact that the granules at the surface have sizes of the order of a few hundred km, whereas convective velocities are of the order of  $1 \text{ km s}^{-1}$ .

(iii) The solar magnetic field is of dipolar nature. A high diffusivity allows the poloidal field lines to get connected across the equator and establish a dipolar parity. Yoshimura et al. (1984) pointed out that a high diffusivity helped in establishing a dipolar parity even in the traditional  $\alpha\Omega$  dynamo models without meridional circulation. This effect becomes more important in flux transport dynamos (Chatterjee et al. 2004). If the diffusivity is low, then the dynamo solutions tend to be quadrupolar and one needs some additional ad hoc assumption like an extra  $\alpha$ -effect at the bottom of the convection zone to make the solutions dipolar (Dikpati & Gilman 2001; Bonanno et al. 2002; Chatterjee et al. 2004). While we observe the generation of the poloidal field on the solar surface by the Babcock–Leighton process (Wang et al. 1989), there is no strong observational evidence for an additional source of poloidal field in the tachocline. A high diffusivity within the convection zone allows us to build models of the solar dynamo with the correct parity without invoking an  $\alpha$ -effect in the tachocline. Dikpati & Gilman (2007) admit that the tachocline  $\alpha$  is a ‘noise-amplifier’. On using mean field equations, they find that transients take very long time to die out. Within the real Sun, there are always fluctuations around the mean and a noise-amplifier would not allow the system to relax to a regular behaviour, especially when the diffusivity is low.

(iv) The irregularities in the solar cycle remain highly correlated in both the hemispheres. In other words, stronger (weaker) solar cycles tend to be stronger (weaker) in both the hemispheres and longer (shorter) solar cycles tend to be longer (shorter) in both the hemispheres. Chatterjee & Choudhuri (2006) studied this problem and concluded that a high diffusivity forces the cycles in the two hemispheres to remain locked with each other even in the presence of asymmetries between the hemispheres. We expect that stochastic fluctuations without having any correlation between the two hemispheres would lead to irregularities correlated in the two hemispheres if the diffusivity is high, but not if the diffusivity is low. This, however, has to be substantiated by detailed simulations, which we are carrying out now. The observed strong correlation of cycle irregularities between the two hemispheres will be impossible to explain with a model having low diffusivity.

All the above arguments taken together suggest a high value of turbulent diffusivity within the solar convection

zone. The turbulent diffusivity seems to have a value such that the diffusion time of the poloidal field across the convection zone turns out to be comparable to the advection time by the meridional circulation. At the first sight, it may seem like a coincidence that these two time scales seem to be so comparable. However, the meridional circulation is supposed to be driven by the turbulent stresses in the convection zone. So both of these two time scales arise from the same physics of turbulence in the convection zone and it may not be so surprising that they are comparable.

It is usually assumed that the meridional circulation plays a very important role in flux transport dynamos. One may wonder if a high diffusivity will reduce the importance of meridional circulation. The poloidal and toroidal fields in flux transport dynamo models are produced at the surface and in the tachocline respectively. These fields are clearly advected by the meridional circulation poleward and equatorward respectively. Since the toroidal field is confined in a narrow layer at the bottom of the SCZ, it is essential to assume a low diffusivity there so that advective effects are more important there than diffusive effects (Choudhuri et al. 2005). A substantially lower diffusivity at the base of the SCZ is assumed both by us (Nandy & Choudhuri 2002; Chatterjee et al. 2004) and by the HAO group (Dikpati & Charbonneau 1999; Dikpati et al. 2004). If diffusive effects were more important than the advective effects, then the dynamo wave at the bottom of SCZ would propagate poleward (Choudhuri et al. 1995), in accordance with the dynamo propagation sign rule (see, for example, Choudhuri 1998, §16.6). In spite of the assumed high diffusivity of our model within the SCZ, there is no doubt that the meridional circulation is responsible for the equatorward propagation of the dynamo wave at the bottom of SCZ and for the poleward advection of the poloidal field at the surface. In the low-diffusivity model of the HAO group, the meridional circulation additionally advects the poloidal field from the solar surface to the tachocline. On the other hand, the poloidal field in our model reaches the tachocline by diffusing from the surface where it is generated.

If cycle 24 turns to be very strong as predicted by Dikpati & Gilman (2006), then that will provide a very convincing argument in favour of low diffusivity, since a high diffusivity will not allow a strong solar cycle just after a weak polar field in the preceding minimum. On the other hand, a weak cycle 24 as predicted by us will make the case for high diffusivity considerably more compelling.

## 6 THE CONNECTION OF THE THEORETICAL MODEL WITH THE OBSERVATIONAL INPUT

In the previous two sections, we have argued that the diffusivity of the poloidal field should be high. With such diffusivity, we expect that the poloidal field generated at the solar surface by the Babcock–Leighton process would diffuse towards the tachocline at all latitudes. Consequently, the approach followed by CCJ of updating the theoretical model with a single number (the value of DM) at the minimum is a drastic simplification. We now discuss how we can feed the observed magnetic field values at different latitudes to update the poloidal field at the minimum.

The code *Surya* calculates the time evolution of  $A(r, \theta, t)$ , whereas the observations provide the line-of-sight component of  $\mathbf{B} = \nabla \times [A(r, \theta, t)\mathbf{e}_\phi]$  at the solar surface. The first step is to use the observational data to calculate  $A(r = R_\odot, \theta, t)$  at the solar surface during the minimum. The relation  $\mathbf{B} = \nabla \times [A(r, \theta, t)\mathbf{e}_\phi]$  implies that the magnetic field has to be divergence-free, which requires that  $\int_0^\pi B_r(r = R_\odot, \theta, t) \sin \theta d\theta$  integrated from one pole to the other must be zero. If errors in magnetic field data make  $\int_0^\pi B_r(r = R_\odot, \theta, t) \sin \theta d\theta$  non-zero, then some special care has to be exercised when calculating  $A(r = R_\odot, \theta, t)$ . We shall discuss this and then point out how we update  $A(r, \theta, t)$  underneath the solar surface.

Following Svalgaard et al. (2005), we operationally define the solar polar field as the net magnetic line-of-sight component measured through the polar most apertures at WSO along the central meridian on the solar disk. We thank Todd Hoeksema for providing line-of-sight magnetic field values averaged over the Carrington Rotation (CR) obtained at WSO for 30 points equally spaced in sine latitude from  $-14.5/15$  to  $+14.5/15$  for each rotation from mid 1976 to 2006 (CR1642–CR2045). The following operations have to be performed to obtain the “real” radial magnetic field from the WSO data (as explained to us by Todd Hoeksema and Leif Svalgaard): (1) the raw data are divided by the cosine of the latitude, (2) a constant scaling factor 1.85 is multiplied to correct the saturation effect, (3) another constant number 1.25 is multiplied to the data of the first two years to correct the scattered light. Thus we may obtain the radial magnetic field for latitude  $-75$  to  $+75$ . What we need is the value from the north pole to the south pole. Svalgaard et al. (1978) pointed out that the variation with latitude of average magnetic flux density between the pole and the polar cap boundary obey the relation of  $\cos^8 \theta$  near the north pole and  $\cos^8(\pi - \theta)$  near the south pole. With this interpolation, we finally obtain the values of  $B_r$  between the two poles. Fig. 10 is the contour of  $B_r$  between latitudes  $\pm 90$  from the middle of 1976 to the end of 2006.

The Sun’s polar field reverses near the maximum of one cycle and then begins its growth toward a new peak with opposite polarity. The polar field becomes strong and well established about three years before the sunspot minimum (Svalgaard et al. 2005). To get  $B_r$  at the minima at the ends of cycles 21, 22 and 23, we average the raw data for the following 3-year periods just before the minima: CR1737–CR1777 (1983:07:10–1986:06:26), CR1871–CR1911 (1993:07:03–1996:06:28) and CR2006–CR2045 (2003:08:02–2006:07:01). For the minimum at the end of cycle 20, however, we only have the data since CR1642 (1976:05:27). Hence, for this case, we average the data for 8 Carrington Rotations, i.e. CR1642–CR1649 (1976:05:27–1976:12:31).

Fig. 11 shows  $B_r$  as a function of latitude at the minima at the ends of cycles 20, 21, 22 and 23. Because of the averaging over 3-year periods, the data look reasonably smooth. However,  $B_r$  does not appear very symmetric at some of the minima. For example, for the minimum at the end of cycle 21, the south polar field is clearly stronger than the north polar field. Since the magnetic field cannot have a monopole component, the flux must be distributed in such a way that  $\int_0^\pi B_r(r = R_\odot, \theta, t) \sin \theta d\theta$  turns out to be zero. The observational data give the following values of this quantity at the ends of the 4 successive minima we are considering: 0.14,

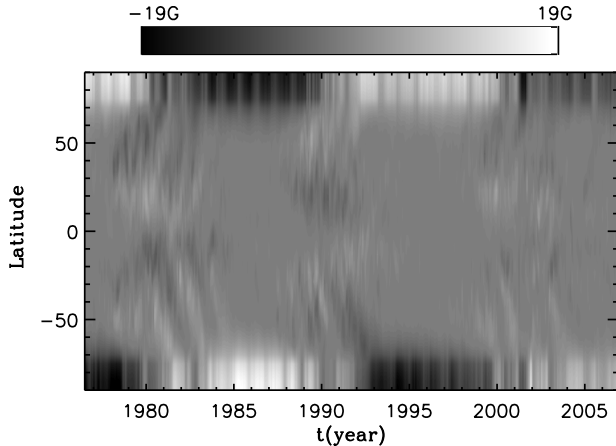


**Figure 10.** Contours of longitude-averaged photospheric magnetic fields from the middle of 1976 to the end of 2006 from WSO polar field data. The values between  $\pm 75$  latitude are given by the observation. The values in the polar regions are extrapolated based on  $\cos^8 \theta$  near the north pole and  $\cos^8(\pi - \theta)$  near the south pole. During the interval Nov. 2000 - Jul. 2002, there were some problems with instrument sensitivity and the real fields are likely to be stronger than that what was recorded (Schatten 2005). However, this does not pose a problem for our theoretical modeling because we require polar field data only during the solar minima.

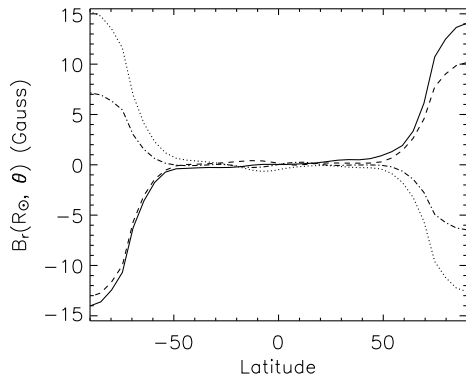


**Figure 11.** The radial magnetic field  $B_r$  for the minima at the ends of cycles 20 (solid line), 21 (dotted line), 22 (dashed line) and 23 (dot-dashed line). This plot is obtained from the WSO data shown in Fig. 10.

-0.001, 0.09 and 0.011 G. These values give an estimate of the monopole component introduced due to the errors in the data. Since this monopole component is not divergence-free, it causes problems when we try to go from  $B_r(r = R_\odot, \theta, t)$  to  $A(r = R_\odot, \theta, t)$ . To have an idea how large the monopole components are at the various minima, keep in mind that a uniform radial field of 1 G over the entire solar surface would make  $\int_0^\pi B_r(r = R_\odot, \theta, t) \sin \theta d\theta$  equal to 2 G.

To calculate  $A(r = R_\odot, \theta, t)$  from  $B_r$ , we use the relation

$$B_r = \frac{1}{r \sin \theta} \frac{\partial}{\partial \theta} (\sin \theta A). \quad (4)$$

If  $A$  is non-zero on any of the poles, then some terms in (1) would become singular. To ensure that  $A$  remains zero at both the poles, we use the following relations to obtain the

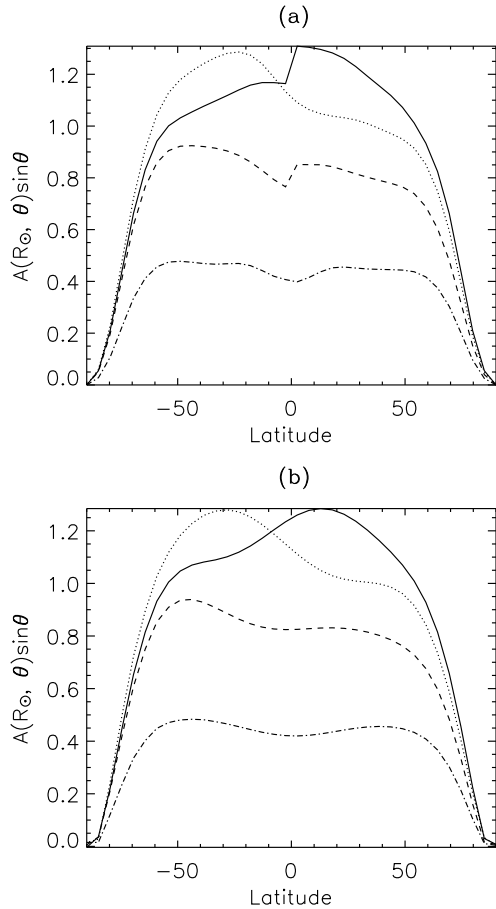
surface values of  $A$  in the two hemispheres:

$$A(R_\odot, \theta, t) \sin \theta = \begin{cases} \int_0^\theta B_r(R_\odot, \theta', t) \sin \theta' d\theta' & 0 < \theta < \frac{\pi}{2} \\ \int_\pi^\theta B_r(R_\odot, \theta', t) \sin \theta' d\theta' & \frac{\pi}{2} < \theta < \pi. \end{cases} \quad (5)$$

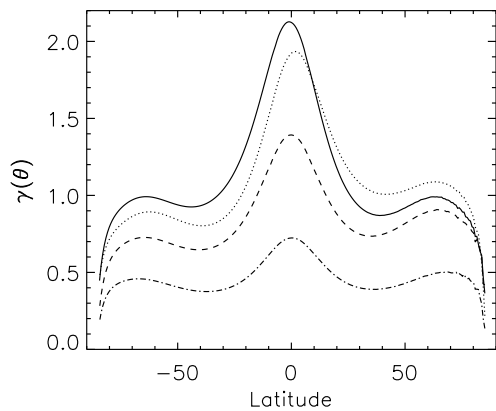
We take  $R_\odot$  as the unit of length in the above expressions giving the numerical value of  $A \sin \theta$ . Only if there is no monopole contribution, we expect  $A(R_\odot, \theta, t)$  calculated in the two hemispheres to match across the equator. Otherwise, we have to connect across the equator by the polynomial fit.

Fig. 12 shows the plots of  $A \sin \theta$  as a function of latitude at the four minima we are considering. The plots before smoothing and after smoothing at the equator are shown in Figs. 12(a) and (b) respectively. Both  $B_r$  plots in Fig. 11 and  $A \sin \theta$  plots in Fig. 12 indicate that the polar field during the minima at the ends of cycles 20 and 21 had nearly the same strength and they were larger than that at the end of cycle 22. The minimum at the end of cycle 23 has the weakest strength. It may be noted that the integrands in (5) have  $B_r$  multiplied by  $\sin \theta$ , which is very small in the polar regions. Hence uncertainties in the value of magnetic field in the polar regions do not have much effect in the computation of  $A \sin \theta$ . In spite of the errors in the data, we find in Fig. 12(a) that the jumps in the plots at the equator are not very large.

We now discuss how the observational data can be fed into the theoretical model to correct for the poloidal field produced at the end of a cycle. We already pointed out that the poloidal field at the minimum produced in our dynamo code corresponds to an average cycle. CCJ identified cycle 23 as an average cycle and took the poloidal field at its beginning as indicative of a poloidal field of average strength in that phase of the dynamo cycle. From the dashed curve in Fig. 11 giving the poloidal field at the end of cycle 22, we find that  $\overline{A \sin \theta}$  averaged over latitude is 0.66. Now, in our dynamo code, the only source of nonlinearity is the magnetic buoyancy and the actual value of  $A \sin \theta$  depends on the critical magnetic field  $B_c$  above which  $B$  is supposed to be buoyant. On setting  $B_c = 108$  G in *Surya*, we find that  $\overline{A \sin \theta}$  at the solar surface averaged over latitude turns out to be equal to 0.66 at the time of minimum in a regular run (taking  $R_\odot$  as the unit of length when calculating  $A$ ). It may be noted that this value of  $B_c$  can be taken as a mean value of the toroidal field beyond which magnetic buoyancy sets in. Flux tube simulations suggest a value of  $10^5$  G inside flux tubes (D'Silva & Choudhuri 1993; Fan et al. 1993), implying a filling factor of order  $10^{-3}$  for the flux tubes. A somewhat larger filling factor of order  $10^{-2}$  was estimated in §3 of Choudhuri (2003). We put  $B_c = 108$  G and run the dynamo code from a minimum to the next minimum, when the poloidal field has to be updated. After stopping the code at a minimum, we check the values of  $A$  at all the grid points on the solar surface. We denote these by  $A_{\text{code}}(R_\odot, \theta)$ . We have already discussed how to obtain  $A$  at a minimum from the observational data and have shown the plots in Fig. 11. Suppose  $A_{\text{code}}(R_\odot, \theta)$  has to be multiplied by  $\gamma(\theta)$  to make the product equal to  $A$  obtained from observational data at that latitude. Fig. 13 shows  $\gamma(\theta)$  as a function of latitude for the four minima we are considering. To avoid the numerical problem of dividing one small number by another, we do not calculate  $\gamma(\theta)$  within 5 degrees of the poles where both  $A_{\text{code}}(R_\odot, \theta)$  and  $A$  become very small. We take  $\gamma(\theta)$  to be 1



**Figure 12.** Poloidal field  $A(R_\odot, \theta) \sin \theta$  inferred from the WSO data (a) before smoothing and (b) after smoothing, for the minima at the ends of cycles 20 (solid line), 21 (dotted line), 22 (dashed line) and 23 (dot-dashed line). It may be noted that  $A(R_\odot, \theta) \sin \theta$  during the minima at the ends of cycles 21 and cycle 23 is negative. We have plotted the absolute values.



**Figure 13.**  $\gamma(\theta)$  at different latitudes for the minima at the ends of cycles 20, 21, 22, 23. The line styles are the same as in Figs. 11 and 12. We do not change values of  $A$  in the polar regions (within 5 degrees of the poles). Hence, there are no values near the poles.

**Figure 14.** (a) The contours of toroidal field and (b) the poloidal field lines, at the solar minimum in an undisturbed run of our *Standard1* model. The solid lines indicate positive values of  $B$  and  $A$ , whereas dotted lines indicate negative values.

within these regions. We now feed the observational data in our theoretical model stopped at the minimum in the following way. At all grid points above  $0.8R_\odot$ , we multiply  $A$  by the factor  $\gamma(\theta)$  appropriate for that latitude. We do not make any changes in the values of  $A$  below  $0.8R_\odot$ . This ensures that the poloidal field in the upper layers, which has been created by the Babcock–Leighton mechanism operating during the previous cycle, gets corrected to the observed values, whereas the poloidal field at the bottom of the convection zone, which may have been created during the still earlier cycles, is left unchanged. Later when we plot the poloidal field lines just after updating, we shall see discontinuities at  $0.8R_\odot$ . However, the discontinuities in the field lines introduced by the discontinuity in  $\gamma(\theta)$  at 5 degrees from the poles are completely insignificant and are not visible in the plots of field lines.

## 7 PREDICTION RESULTS

We have described in the previous section how the observational data of the poloidal field can be fed into the theoretical dynamo model stopped at a minimum, to correct for the randomness in the poloidal field generation process. We obtain a relaxed solution of our *Standard1* model with our code *Surya* and stop it at a minimum. Identifying this as the minimum at the end of cycle 20, we update the poloidal field by feeding observational data appropriate for this minimum. Then we run the code in successive steps of one cycle, stopping at the consecutive minima to update the poloidal field by feeding the observational data. The run after the minimum at the end of cycle 23 generates the prediction for cycle 24.

Fig. 14 gives the contours of toroidal field and the poloidal fields lines at a minimum during a regular run of *Surya* for the *Standard1* model. Since the diffusivity is low within the tachocline where the toroidal field is produced, we find that the toroidal fields from the previous cycles are still present. It will be seen that our theoretical butterfly diagrams show eruptions from the previous cycle even after a new cycle has begun. Our best theoretical models for the solar cycle still suffer from this defect. On the other hand, the high diffusivity of the poloidal field within the convection zone makes the poloidal fields produced in earlier cycles decay away and we predominantly have the poloidal field produced in the previous cycle present at the time of the minimum. Fig. 15 shows poloidal field lines at the four minima just after they have been updated by feeding the observational data. It is clear that the poloidal field tends to be asymmetric between the hemispheres. For example, the poloidal field at the end of cycle 20 appears stronger in the northern hemisphere. This is consistent with Fig. 11, where we see that the north polar field was stronger than the south polar field during the minimum at the end of cycle 20. We see discontinuities in poloidal field lines at  $r = 0.8R_\odot$

**Figure 15.** The poloidal field lines given by constant contours of  $Ar \sin \theta$  just after correcting by the observational data during the minima at the ends of cycles (a) 20, (b) 21, (c) 22 and (d) 23. The dashed lines correspond to  $r = 0.8R_{\odot}$ .

in Fig. 15. These discontinuities get smoothed as our code advances the magnetic field for a few weeks and cause no problems. An alternative procedure is to multiply  $A$  at all depths by  $\gamma(\theta)$ . We have checked that this gives very similar result for our high-diffusivity model, where we do not have poloidal fields created in the earlier cycles stored at the bottom of SCZ. However, one gets considerably different results if these different procedures are followed in a low-diffusivity model. A very careful comparison of the poloidal field lines in Fig. 14 with the field lines above  $0.8R_{\odot}$  in the four plots in Fig. 15 shows that the field lines connect across the equator more smoothly in Fig. 15 (i.e. the field lines appear more bent in Fig. 14). In other words, poloidal field lines reconstructed from observational data suggest slightly more diffusion between the two hemispheres compared to the field lines from the pure theoretical model shown in Fig. 14. This can be taken as another evidence that the magnetic diffusivity assumed by us is not unreasonable. If anything, the comparison of field lines in Figs. 14 and 15 suggests that the actual diffusivity may even be higher than what we are using in our theoretical model.

Fig. 16 now presents our results for cycles 21–24 generated by our methodology. The top panel superposes the monthly sunspot number generated from our model (solid line) on the observational data (dashed line). We may point out that the absolute value of the theoretical sunspot number from our numerical code does not have any particular significance, since a finer grid would make  $B$  buoyant at a larger number of grid points and will increase the number of eruptions in our method of treating magnetic buoyancy. To generate the top panel of Fig. 16, we scaled the theoretical sunspot number suitably to make it fit the observational plot. The bottom panel shows the butterfly diagram produced by our model. We see in the top panel that the theoretical plot is in quite good agreement with the observational data for cycles 22–23. The fit is not so good for cycle 21. One possible reason for this is the incompleteness of the poloidal field data at the end of cycle 20. The data are available only from the middle of that minimum and there were some calibration problems in the first 2 years. The other possibility is that, after we initialize the code by feeding observational data at a minimum, it may take about a cycle before the code starts giving really reliable outputs. The cycle 24 comes out as the weakest cycle in a long time.

The relative total sunspots numbers for cycles 21–24 produced by the model are 3866, 3862, 3300 and 2292, respectively. Hence, the coming cycle 24 should be 30.5% weaker than cycle 23, which makes cycle 24 a little stronger than what it was in the earlier calculation of CCJ, who found cycle 24 to be about 35% weaker compared to cycle 23. We do believe that the methodology adopted in this paper is a more realistic, thorough and reliable methodology. However, the advantage of the methodology of CCJ is that this methodology, based on using a single number like the value of DM to update the poloidal field at the minimum, is ex-

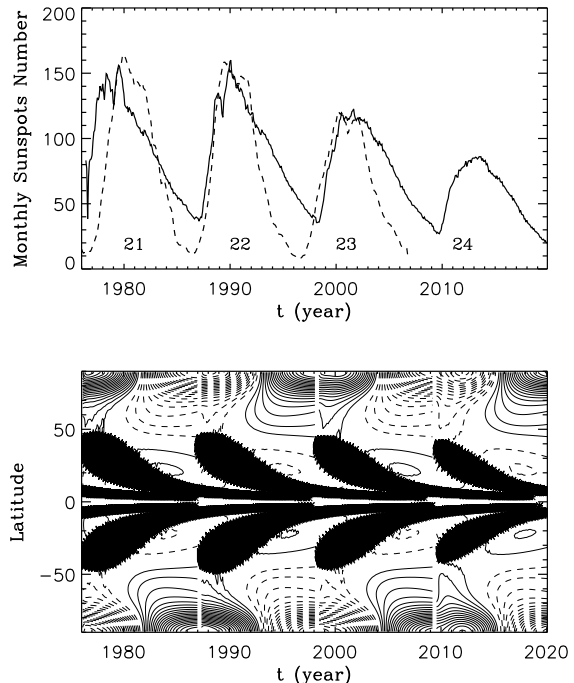


**Figure 16.** The upper panel shows the theoretical monthly smoothed sunspot number (solid line) superposed on the monthly smoothed sunspot numbers from observation (dashed line). For cycles 22 and 23, the two lines match quite well. But for cycle 21, the result from the model is slightly weaker than the observational result. Incomplete observational data at the end of cycle 20 might be the reason. The cycle 24 is clearly very weak. The lower panel shows the theoretical butterfly diagram of sunspots superimposed on the contours of radial field for the cycles 21–24. The solid and dashed curves in the lower panel indicate positive and negative values of  $B_r$  at the surface. (Note that the solid and dashed curves got accidentally interchanged in Fig. 3 of CCJ.)

tremely easy and straightforward to implement in a dynamo model. The fact that the two methodologies give reasonably similar results suggests that the simple method of CCJ can be used for a quick first calculation of solar cycles, to give reasonably reliable results.

One additional advantage of our present methodology over the methodology of CCJ is that the present methodology allows us to study the asymmetry between the two hemispheres, which was not possible with the methodology of CCJ. The North-South asymmetry can be defined as

$$AS = \frac{N - S}{[N + S]_{ave}}, \quad (6)$$

where  $N$  and  $S$  stand for the annual sunspot group numbers in northern and southern hemisphere respectively (Li et al. 2002), and  $[N + S]_{ave}$  is the value of  $N + S$  averaged over certain interval, which we take here to be 1976–2006. Different observational manifestations of solar activity, such as major flares, sunspot numbers, sunspot area data and so on, indicate that the solar activity can be asymmetric about the equator. Fig. 17a shows the asymmetry  $AS$  of yearly sunspot area during 1976–2006. Fig. 17b gives the asymmetry from our theoretical model. At the first sight, it may seem that the theory does not match observations well. The main reason

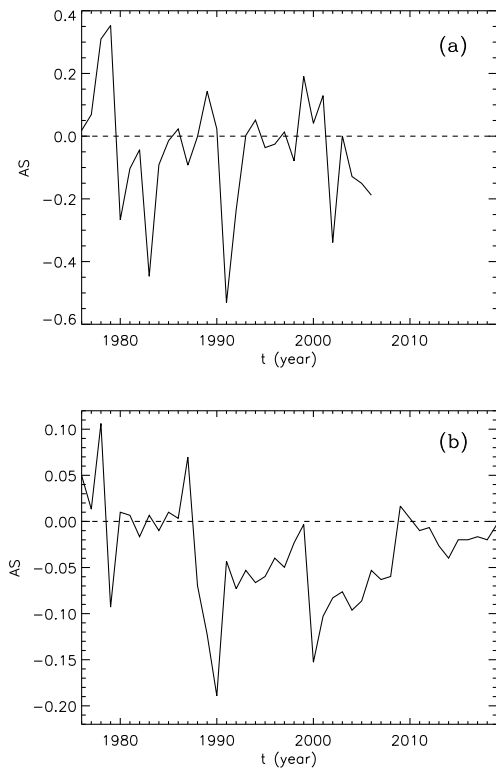


**Figure 17.** (a): Asymmetry  $AS$  of yearly sunspots area from the observational data. (b): Asymmetry  $AS$  of yearly sunspots number from the theoretical model.

why the two plots look so different is that the observational data is much noisier than the theoretical result. It may be noted that our method of treating magnetic buoyancy introduces some noise in the sunspot number, as can be seen in the top panel of Fig. 16. When we used the non-local method of treating magnetic buoyancy in our calculations with the low-diffusivity model in §4, the theoretical sunspot numbers turned out to be much smoother (see Fig. 9). Also, in our theoretical model, we are including the cumulative effect of random fluctuations by updating the poloidal field at the minima. However, the random fluctuations in the real solar cycle data are much larger than in the theoretical model, which makes Fig. 17a and Fig. 17b look different. To show that the theory matches the observations much better on filtering out the noise, we apply the following procedure both to the theoretical and observational data. We calculate the 5-year running average of  $N$  and  $S$  such that the values of these in the year  $y$  are taken to be averages from the year  $y - 2$  to  $y + 2$ . Then we calculate  $AS$  using these running averages. Fig. 18 shows the theoretical plot (solid line) superposed on the observational data (dashed line). We now see a much better agreement between theory and observations. The maximum values of  $|AS|$  are now comparable in the observational and theoretical plots, which was not the case before smoothing as can be seen in Fig. 17.

It is not difficult to understand why  $AS$  in the theoretical model tends to be negative after 1987. During the minimum at the end of cycle 21 (i.e. around 1986), the south polar field was stronger than the north polar field, as can be

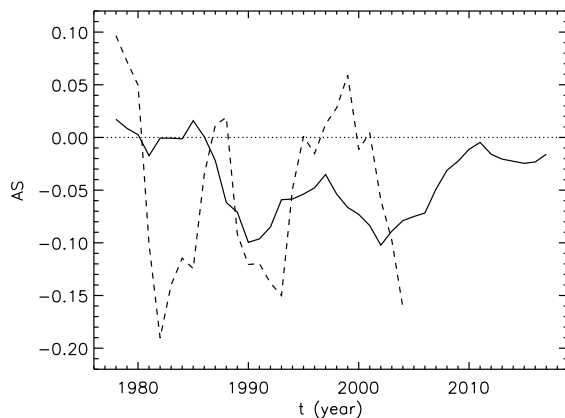


**Figure 18.** The hemispheric asymmetries shown in Fig. 17 are now smoothed by using 5-year running means of  $A$  and  $S$  before calculating  $AS$ . The theoretical result (solid line) is superposed on the observational result (dashed line).

seen in Figs. 11 and 12. This has clearly made the southern hemisphere more active during the next cycle, leading to a tendency of  $AS$  being negative. During the minima at the ends of cycles 22 and 23 also, the south polar field has been marginally stronger than the north polar field, although the asymmetry has not been as pronounced as at the end of cycle 21. Our theoretical model suggests that the tendency of  $AS$  being negative will continue in cycle 24, although this tendency will not be as strong as it was during the period 1987–2006. This is a very clear prediction and it will be interesting to see if this prediction turns out to be true or not. We see in Fig. 18 that the observational value of  $AS$  tended to be negative during 1988–2005 in agreement with theoretical results. We may also point out that the north polar field was stronger at the end of cycle 20 (i.e. around 1976), which can be seen in Figs. 11 and 12. This led to a tendency of  $AS$  being positive during the next maximum around 1979, which is seen in Fig. 18 both in the theoretical model and in the observational data.

We would like to stress that the quality of the polar field data is very important in carrying out the calculations we have reported in this Section. We have repeated our calculation of cycles 21–24 using the NSO data of polar magnetic field (provided by David Hathaway) in addition to the WSO data we have been using. We find that there is no good agreement between the theoretical results and observational data for the past cycles 21–23 if we use the NSO data. We get a good agreement only when we use the WSO data.

## 8 CONCLUSION

Since any theoretical investigation of a complex system like the solar dynamo should be guided by observational data, we began by looking at the observational data carefully. Although systematic direct measurements of the Sun's polar field are available only from mid-1970s, other kinds of proxies throw some light on the polar field at earlier times. We saw that there is reasonably good evidence that the strength of the cycle  $n + 1$  is strongly correlated with the polar field

at the end of cycle  $n$ , giving credence to the method of predicting solar cycles by using the polar field at the preceding minimum as a precursor (Svalgaard et al. 2005, Schatten 2005). On the other hand, the polar field at the end of a cycle is not correlated with the strength of the cycle. These observational facts guide us in developing our theoretical approach.

We suggest that the lack of correlation of the polar field at the end of a cycle with the strength of the cycle, as seen in Fig. 3, is a compelling evidence that the generation of the poloidal field involves randomness. Since the poloidal field is produced by the Babcock–Leighton mechanism, the physical origin of this randomness is not difficult to understand. The tilts of bipolar sunspots on the solar surface have a large scatter around the mean given by Joy’s law, presumably caused by the interaction of the rising flux tubes with the convective turbulence in the uppermost layers of SCZ (Longcope & Choudhuri 2002). Since the poloidal field produced in the Babcock–Leighton process depends on the tilt, this scatter in tilts undoubtedly would introduce a randomness. CCJ proposed that the theoretical dynamo model should be corrected by feeding the actual data of poloidal field produced at the end of a cycle when we want to model actual solar cycles. We have followed this procedure in the present work as well.

As for the strong correlation between the polar field at a minimum and the strength of the next cycle, the theoretical explanation depends on the fact that the poloidal field is transported to the tachocline and then stretched by differential rotation to produce the toroidal field responsible for the strength of the cycle. Since these are regular and deterministic processes, we expect a causal link to persist. However, in low-diffusivity dynamo models ( $\eta \approx 10^{10} \text{ cm}^2 \text{ s}^{-1}$ ), the polar field can be transported to the tachocline only by meridional circulation and the advection time is too large to explain the correlation between the polar field and the immediate next cycle. Only in high-diffusivity models ( $\eta \approx 10^{12} \text{ cm}^2 \text{ s}^{-1}$ ), the poloidal field created in the previous cycle gets advected to the pole and simultaneously diffuses to the tachocline, leading to the observed correlation. We have provided several other arguments that the solar dynamo has to be a high-diffusivity dynamo.

CCJ had used a single number (the value of DM) to feed the polar field at the minimum into the theoretical model. We now have developed a methodology of feeding the detailed information of the poloidal field at different latitudes. While this is a much more satisfactory method than the method used by CCJ, we find that the method of CCJ also gives results in qualitative agreement with the more detailed method. Since the method of CCJ is much easier to implement, it can be used to obtain a quick first result. It should be kept in mind that the prediction of the sunspot maximum at the beginning of the cycle is possible only because the rising phase is dominated by fairly ordered and deterministic processes like the advection/diffusion of the poloidal field and the generation of the toroidal field by differential rotation. The declining phase of the cycle, when the poloidal field is produced by the Babcock–Leighton process, involves randomness and is not predictable. If this view is correct, then we can think of predicting a cycle only after the declining phase of the previous cycle is over and we know from observations how much poloidal field has been

produced. It may thus never be possible to make a realistic prediction of the strength of a sunspot maximum more than 7–8 years ahead in time. Bushby & Tobias (2007) have given several other arguments to show the impossibility of long-term prediction in the solar dynamo.

A high-diffusivity dynamo certainly has a shorter memory compared to a low-diffusivity dynamo. Additionally, when the poloidal field information is fed into the theoretical model at the time of the minimum, that also tries to erase the memory of the dynamo. One important question is whether the memory of the dynamo is restricted to be less than 11 years in our model, since the poloidal field is updated after every 11 years. Fig. 2 of CCJ showed that the memory of a disturbance can persist for at least 2 cycles if the dynamo is not disturbed any more after giving a single kick. Will the introduction of randomness after a cycle erase this memory completely? The answer will depend on really how random the next kick is. There is no doubt that the Babcock–Leighton process introduces randomness in the generation of the poloidal field. However, the limited data shown in Fig. 3 is insufficient for us to conclude whether the randomness is serious enough to erase the memory completely or whether some weak correlation still exists between the strength of a cycle and the poloidal field produced at its end.

Svalgaard et al. (2005) suggested a simple relation that the maximum International Sunspot Number  $R_{max}$  of cycle  $n$  will be proportional to the value of DM at the end of cycle  $n - 1$ , i.e.

$$(R_{max})_n = k(DM)_{n-1}. \quad (7)$$

This implies a complete loss of memory of the previous cycles. If the randomness introduced in the Babcock–Leighton process does not completely erase the memory of the immediately preceding cycle, then, on the basis of Fig. 2 of CCJ showing that the memory of the polar field can persist for a couple of cycles, we would expect a more complicated functional relationship

$$(R_{max})_n = f[(DM)_{n-1}, (DM)_{n-2}]. \quad (8)$$

For the last few cycles, the results obtained with our dynamo model are roughly in agreement with what one would expect on the basis of (7). However, if two preceding cycles have been of very unequal strengths and (8) is the correct relation rather than (7), then it is possible that a detailed calculation based on a dynamo model may give a result significantly different from what one would get from (7). The theoretical sunspot number shown in Fig. 16 also indicates that (8) may be a more correct relation. Since we had not fed any information about the minimum at the end of cycle 19 into our theoretical model, the theoretical cycle 21 does not match observations so well as the cycles 22–23 for which data for the 2 previous minima had been fed.

One important question is whether observational data can help us in deciding about the memory of the dynamo process. We see in Fig. 2 that the solid circles based on actual polar field measurements lie close to a straight line, suggesting that (7) may actually be true. However, the open circles based on more uncertain data show a scatter. We cannot be sure whether this scatter is due to the errors in the data or whether there is an inherent scatter in the data. If there is an inherent scatter, one possible explanation is that

(8) is the correct relation and that is why we do not expect all data points in a  $(R_{max})_n$  versus  $(DM)_{n-1}$  plot to lie on a straight line or a curve. An alternative explanation, however, is also possible. We have been tacitly assuming that the transport of the poloidal field to tachocline and its stretching by differential rotation there are ordered and deterministic processes. As argued by Choudhuri (2003), the magnetic field has to become intermittent at some stage to account for the existence of flux tubes. This also may introduce some randomness, making a departure from a strict causal relationship between  $(R_{max})_n$  and  $(DM)_{n-1}$ .

Sometimes the so-called ‘even-odd rule’ is forwarded as an argument in favour of the dynamo having a memory lasting for at least 2 cycles. There have been 6 consecutive pairs of cycles in which the odd cycle was stronger than the preceding even cycle. The cycle 23 broke this ‘even-odd rule’ after more than a century. It is difficult to be sure whether the ‘even-odd rule’ really exists or whether this apparent effect was caused by the accident of statistics. Charbonneau et al. (2007) have made the provocative suggestion that this effect is caused by the period doubling in the dynamo, which is a nonlinear chaotic system. If this theoretical explanation is correct, then the randomness introduced in the Babcock–Leighton process should not erase the memory of the preceding cycle completely.

To sum up, there is no doubt that the Babcock–Leighton process of poloidal field generation introduces a significant amount of randomness in the dynamo process and this has to be corrected in a theoretical model by using actual observational data. Whether this process erases all the memory of previous cycles or whether some memory still persists is a question which cannot be settled on the basis of currently available limited observational data. Perhaps we should keep our minds open and allow for the possibility that the dynamo retains some memory even after the Babcock–Leighton process introduces a significant element of randomness.

Our model makes a very clear prediction that cycle 24 will be a rather weak cycle. This is a quite robust prediction even if the memory of the dynamo persists for a few years beyond one cycle, since the polar fields at the ends of both cycles 22 and 23 have been weak. In our high-diffusivity dynamo model, it would be completely impossible to have a weak polar field (like what we have now) to be followed by a very strong cycle as predicted by Dikpati & Gilman (2006). Apart from the fact our two dynamo models used diffusivities differing by a factor of 50, the second main difference is that Dikpati & Gilman (2006) have taken the sunspot area data as the source of the poloidal field. In our view, the poloidal field generation involves randomness and cannot be calculated deterministically from sunspot number or area data of previous cycles. We now have to wait for a verdict on this debate from the Sun-god himself in about 4–5 years’ time.

## ACKNOWLEDGMENTS

We are grateful to Dirk Callebaut, David Hathaway, Todd Hoeksema, Ken Schatten, Leif Svalgaard and Andrey Tlatov for explaining various aspects of observational data. We thank Axel Brandenburg, Paul Charbonneau and Dibyendu

Nandy for valuable discussions. We also acknowledge discussions with Mausumi Dikpati during our efforts in reproducing her low-diffusivity model. Suggestions from the referee, Leif Svalgaard, and the Editor helped in improving the presentation. This work began when A.R.C. was a Visiting Professor at the National Astronomical Observatories in Beijing. He would like to thank Jingxiu Wang, Jun Zhang and other members of the group for the very warm hospitality. J.J. acknowledges financial support from National Basic Research Program of China through grant nos. 2006CB806303, 10573025 and 10603008. P.C. acknowledges financial support from C.S.I.R through grant no. 9/SPM-20/2005-EMR-I.

## REFERENCES

- Babcock H. W., 1961, *ApJ*, 133, 572  
 Babcock H. W., Babcock H. D., 1955, *ApJ*, 121, 349  
 Bonanno A., Elstner D., Rüdiger G., Belvedere G., 2002, *A&A*, 390, 673  
 Bushby P. J., Tobias S. M., 2007, arXiv:0704.2345v1  
 Cameron R., Schüssler M., 2007, *ApJ*, 659, 801  
 Charbonneau P., Beaubien G., St-Jean C., 2007, *ApJ*, 658, 657  
 Charbonneau P., Dikpati M., 2000, *ApJ*, 543, 1027  
 Chatterjee P., Choudhuri A. R., 2006, *Sol. Phys.*, 239, 29  
 Chatterjee P., Nandy D., Choudhuri A. R., 2004, *A & A*, 427, 1019  
 Choudhuri A. R., 1989, *Sol. Phys.*, 123, 217  
 Choudhuri A. R., 1990, *ApJ*, 355, 733  
 Choudhuri A. R., 1992, *A&A*, 253, 277  
 Choudhuri A. R., 1998, *The Physics of Fluids and Plasmas: An Introduction for Astrophysicists*, Cambridge University Press  
 Choudhuri A. R., 2003, *Sol. Phys.*, 215, 31  
 Choudhuri A. R., 2005, *The User’s Guide to the Solar Dynamo Code Surya* (available on request)  
 Choudhuri A. R., 2007a, *Adv. Space Res.* (in press)  
 Choudhuri A. R., 2007b, *J. Astrophys. Astron.* (submitted)  
 Choudhuri, A. R., Chatterjee, P., Jiang, J., 2007, *Phys. Rev. Lett.*, 98, 131101  
 Choudhuri A. R., Chatterjee P., Nandy D., 2004, *ApJ*, 615, L57  
 Choudhuri A. R., Gilman P. A., 1987, *ApJ*, 316, 788  
 Choudhuri A. R., Konar S., 2002, *MNRAS*, 332, 933  
 Choudhuri A. R., Nandy D., Chatterjee P., 2005, *A&A*, 437, 703  
 Choudhuri A. R., Schüssler M., Dikpati M., 1995, *A&A*, 303, 29  
 Dikpati M., Charbonneau P., 1999, *ApJ*, 518, 508  
 Dikpati M., de Toma G., Gilman P., 2006, *Geo. Res. Lett.*, 33, L05102  
 Dikpati M., de Toma G., Gilman P. A., Arge C. N., White O. R., 2004, *ApJ*, 601, 1136  
 Dikpati M., Gilman P. A., 2001, *ApJ*, 559, 428  
 Dikpati M., Gilman P. A., 2006, *ApJ*, 649, 498  
 Dikpati M., Gilman P. A., 2007, *Sol. Phys.*, 241, 1  
 D’Silva S., Choudhuri A. R., 1993, *A&A*, 272, 621  
 Durney B. R., 1995, *Sol. Phys.*, 160, 213  
 Fan Y., Fisher G. H., Deluca E. E., 1993, *ApJ*, 405, 390  
 Gizon L., 2004, *Sol. Phys.*, 224, 217  
 Guerrero G., de Gouveia Dal Pino E. M., 2007, *A&A*, 461, 341  
 Hathaway D. H., Nandy D., Wilson R. M., Reichmann E. J., 2003, *ApJ*, 589, 665  
 Hoyng P., 1993, *A&A*, 272, 321  
 Köhler H., 1973, *A & A*, 25, 407  
 Konar S., Choudhuri A. R., 2004, *MNRAS*, 348, 661  
 Leighton, R. B., 1969, *ApJ*, 156, 1  
 Li K. J., Liu X. H., Yun H. S., et al., 2002, *Publ. Astron. Soc. Japan.*, 54, 629  
 Longcope D. W., Choudhuri A. R., 2002, *Sol. Phys.*, 205, 63  
 Longcope D. W., Fisher G. H., 1996, *ApJ*, 458, L380



- Makarov V. I., Makarova V. V., Sivaraman K. R., 1989, *Sol. Phys.*, 119, 45
- Makarov V. I., Tlatov A. G., Callebaut D. K., Obridko, V. N., Shelting, B. D., 2001, *Sol. Phys.*, 198, 409
- Mininni P., Gomez D. O., 2002, *ApJ*, 573, 454
- Moffatt H. K., 1978, *Magnetic Field Generation in Electrically Conducting Fluids*, Cambridge University Press
- Moss D., Brandenburg A., Tavakol R., Tuominen I., 1992, *A&A*, 265, 843
- Nandy D., Choudhuri A. R., 2001, *ApJ*, 551, 576
- Nandy D., Choudhuri A. R., 2002, *Sci*, 296, 1671
- Ossendrijver A. J. H., Hoyng P., Schmitt D., 1996, *A&A*, 313, 938
- Parker E. N., 1955, *ApJ*, 122, 293
- Parker E. N., 1979, *Cosmical Magnetic Fields*, Oxford University Press
- Schatten K., 2005, *Geo. Res. Lett.*, 32, L21106
- Schatten K. H., Scherrer P. H., Svalgaard, L., Wilcox, J. M., 1978, *Geo. Res. Lett.*, 5, 411
- Sheeley N. R. Jr., 1991, *ApJ*, 374, 386
- Spruit H. C., 1974, *Sol. Phys.*, 34, 277
- Steenbeck M., Krause F., Rädler K. H., 1966, *Z Naturforsch*, 21, 369
- Svalgaard L, Cliver E. W., Kamide Y., 2005, *Geo. Res. Lett.*, 32, L01104
- Svalgaard L, Duvall, T. L., Scherrer, P. H., 1978, *Sol. Phys.*, 58, 225
- van Ballegooijen A. A., Choudhuri A. R., 1988, *ApJ*, 333, 965
- Wang Y.-M., Nash A. G., Sheeley N. R. Jr, 1989, *ApJ*, 347, 529
- Wang Y.-M., Sheely, N. R., Jr., 1989, *Sol. Phys.*, 124, 81
- Wang Y.-M., Sheeley N. R. Jr, Nash A. G., 1991, *ApJ*, 383, 431
- Yoshimura H., Wang Z., Wu F., 1984, *ApJ*, 280, 865